Proceedings of Symposia in Applied Mathematics

A Hybrid Scheme for Flows in Porous Media

Smadar Karni and Gerardo Hernández-Dueñas

Abstract. The Baer-Nunziato model is used to describe the flow of compressible gas in a porous bed. We are concerned with flows in which the porosity changes discontinuously across a so-called compaction wave, and consider the related Riemann problem. A recent study [**CAL**] has illustrated the failure of various numerical schemes to compute correct solutions across compaction waves. The errors were linked to the failure of the scheme to maintain constant entropy across the interface. We propose a hybrid strategy that reverts to a nonconservative formulation across the porosity jump and solves directly for the entropy. The formulation trivially respects the jump conditions, and may be combined with one's preferred conservative scheme away from the interface. Numerical tests illustrate the merits of this strategy.

1. Introduction

The Baer-Nunziato (BN) model is given by

$$
\begin{aligned}
&(\rho_g\phi_g)_t + (\rho_g\phi_g u_g)_x = 0\\
&(\rho_g\phi_g u_g)_t + (\rho_g\phi_g u_g^2 + p_g\phi_g)_x = p_g(\phi_g)_x\\
&(E_g\phi_g)_t + (u_g(\phi_g E_g + \phi_g p_g))_x = p_g u_s(\phi_g)_x\\
&(\rho_s\phi_s)_t + (\rho_s\phi_s u_s)_x = 0\\
&(\rho_s\phi_s u_s)_t + (\rho_s\phi_s u_s^2 + p_s\phi_s)_x = p_g(\phi_s)_x\\
&(E_s\phi_s)_t + (u_s(\phi_s E_s + \phi_s p_s))_x = p_g u_s(\phi_s)_x\\
&(\phi_s)_t + u_s(\phi_s)_x = 0
\end{aligned}
\tag{1.1}
$$

Here $\rho,\ u,\ p$ and E denote the density, velocity, pressure and energy of the respective phases, both assumed ideal and satisfy the Equation of State (EOS)

$$
E = \frac{1}{2}\rho u^2 + \frac{p}{\gamma - 1} \tag{1.2}
$$

Key words and phrases. Multi-phase flow; Nonconservative systems, Riemann problems; Work supported in part by NSF DMS #0609766 and CONACyT #160147.

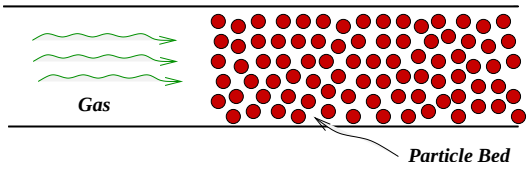

FIGURE 1. Compressible flow in a gas permeable particle bed

and ϕ is the porosity, satisfying

$$\phi_g + \phi_s = 1 \ . \tag{1.3}$$

The BN model was originally proposed to describe flame propagation in gas-permeable reactive granular materials [**BN**]. Here the terms due to combustion processes, drag and heat transfer are neglected. It is an averaged two-phase flow model, expressing mass conservation, and momentum and energy balance of the gas and solid phases. The last equation governs the evolution of the porosity. The system is nonconservative due to momentum and energy exchange between the phases. The underlying conservation is revealed upon addition of the momenta (energy) equations of the individual phases. The presence of the non-conservative terms has major consequences both theoretically and computationally . The eigenvalues of system (1.1) are given by

$$u_g - c_g, u_g, u_g + c_g, u_s - c_s, u_s, u_s, u_s + c_s \tag{1.4}$$

corresponding to familiar waves in the Euler subsystems of the respective phases, and an additional so-called compaction wave that carries changes in porosity and propagates with the speed of the solid phase, u_s. Here $c = \sqrt{\gamma p/\rho}$ denotes the speed of the sound.

We are interested in flows where the porosity is piecewise constant (See the schematic in Figure 1). In this case, the system reduces to two single-phase Euler subsystems which "talk" to each other through a set of jump conditions that hold across the porosity jump. The jump conditions across the porosity jump may be obtained using the Riemann Invariants (see, for example [**BN, CAL, AW2**]),

$$u_s, \ \eta_g, \ \eta_s, \ \phi_g\rho_g v_g, \ \phi_g p_g + \phi_s p_s + \phi_g\rho_g v_g^2, \ \frac{1}{2}v_g^2 + \frac{c_g^2}{\gamma - 1} \tag{1.5}$$

all of which do not change across the porosity jump. Here, $\eta = p/\rho^\gamma$ denotes the entropy, $v_g = u_g - u_s$ denotes the speed of the gas relative to the speed of the compaction wave. The system is only conditionally hyperbolic, and may fail to have a complete set of eigenvectors if

$$(u_s - u_g)^2 = c_g^2 \tag{1.6}$$

In the special case where the particle bed is stationary, $u_s = 0$, and the solid phase is assumed incompressible, system (1.1) reduces to

$$\begin{aligned} (\rho\phi)_t \quad &+ \quad (\rho\phi u)_x = 0 \\ (\rho\phi u)_t \quad &+ \quad (\rho\phi u^2 + \phi p)_x = p\phi_x \\ (\phi E)_t \quad &+ \quad (u(\phi E + \phi p))_x = 0, \end{aligned} \tag{1.7}$$

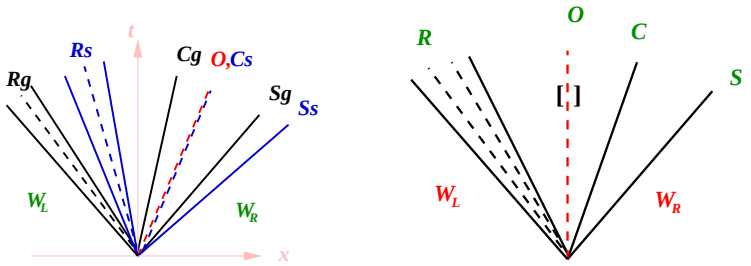

FIGURE 2. Schematic of the Riemann problem for the BN system (1.1) (left) and for the reduced system (1.7) (right).

which is effectively the Euler equations with area variation, where the porosity $\phi = \phi(x)$ may be identified with the cross sectional area. Here, the subscript $(\cdot)_g$ has been omitted.

The jump conditions across the stationary porosity jump are

$$[\phi\rho u] = 0,\ [\eta] = 0,\ [h] = 0. \tag{1.8}$$

Here $h = \frac{1}{2}u^2 + \frac{c^2}{\gamma - 1}$ is the specific enthalpy.

Figure 2 illustrates a typical solution of the Riemann problem consisting of rarefactions (R), shocks (S), contact waves (C) and a compaction wave (O). We note that although a compaction wave propagates with the solid phase velocity u_s, it is *not* a contact wave. This is easily appreciated in the stationary case. Using (1.8) a simple calculation confirms that

$$[p] = 0 \implies [\rho] = 0 \implies [u] = 0 \implies [\phi] = 0$$

provided $u \neq 0$, indicating that unlike a contact wave, across a compaction wave ($[\phi] \neq 0$) the pressure does not remain constant ($[p] \neq 0$) .

We further note that for the BN system (1.1), the two dimensional eigenspace corresponding to u_s may be spanned by one eigenvector describing a pure solid contact and another describing a compaction wave. The overall jump in the solution across this wave front is, of course, a combination of the respective jumps.

2. A Hybrid Approach

Solutions for the Riemann problem may be nonunique [**AW1, AW2, SWK**]. Even when unique, they may be difficult to compute. Computations based on the conservative formulation (1.1) were shown to have difficulties maintaining constant entropy across the porosity jump, resulting in incorrect jump in the solution [**CAL**].

Using a conservative formulation is of course necessary when shocks are present. However, looking beyond conservative formulations has proved beneficial in various other contexts. For example, using a pressure-based formulation to compute propagating material interfaces [**AK**] or using equilibrium variables to compute accurate steady-state solutions to shallow water systems [**NXS, GR**]. We focus first on the reduced system (1.7). Note that if instead of recovering the entropy from the conserved variables one solves for the entropy directly using the entropy evolution equation

$$\eta_t + u\eta_x = 0 \tag{2.1}$$

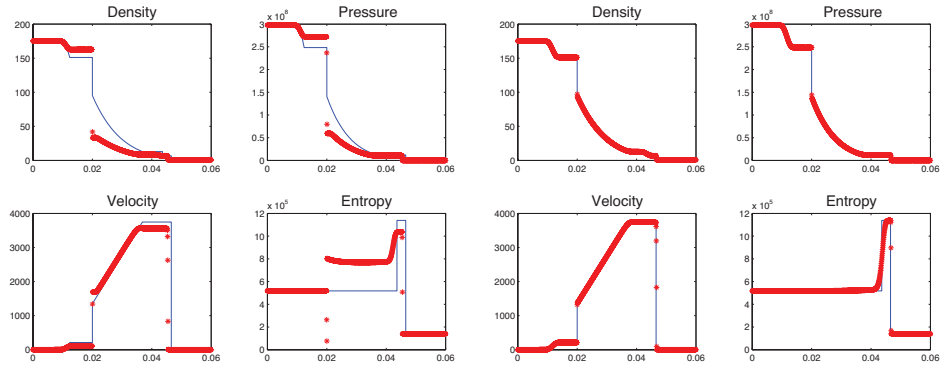

FIGURE 3. Computed and exact solutions corresponding to shock-tube data (3.2): conservative (left) and hybrid (right) formulations

then if η is constant in the data ($\eta_x = 0$), it will automatically remain constant in the solution ($\eta_t = 0$). Any method based on a consistent discretization of (2.1) will inherit this property. This seems to indicate that (2.1) is a suitable equation to use across the porosity jump where $[\eta] = 0$. Based on this observation, we propose a hybrid strategy:

(i) Away from the porosity jump solve

$$\begin{aligned} (\phi\rho)_t + (\phi\rho u)_x &= 0 \\ (\phi\rho u)_t + (\phi\rho u^2 + \phi p)_x &= p\phi_x \\ (\phi E)_t + (u(\phi E + \phi p))_x &= 0 \end{aligned}$$

(ii) Across the porosity jump solve

$$\begin{aligned} (\phi\rho)_t + (\phi\rho u)_x &= 0 \\ \eta_t + u\eta_x &= 0 \\ (\phi E)_t + (u(\phi E + \phi p))_x &= 0 \end{aligned}$$

We note that the energy flux may be written as $\phi\rho uh$. It is straightforward to see that if the data correspond to a porosity wave, hence satisfy (1.8), the above nonconservative formulation based on the entropy equation will recognize and respect this solution. We also point out that in this hybrid approach the conservative formulation is only used away from the porosity jump, and while technically it has a nonconservative term on its right hand side, that term in fact vanishes and the system reduces to effectively the standard Euler system.

The eigenvectors of the above conservative and nonconservative formulations are given respectively by

$$R^C = \begin{pmatrix} 1 & 1 & 1 \\ u-c & u & u+c \\ h-uc & \frac{1}{2}u^2 & h+uc \end{pmatrix} \qquad R^{NC} = \begin{pmatrix} 1 & 1 & 1 \\ 0 & -\frac{\gamma\eta}{\phi\rho} & 0 \\ h-uc & \frac{1}{2}u^2 & h+uc \end{pmatrix}$$

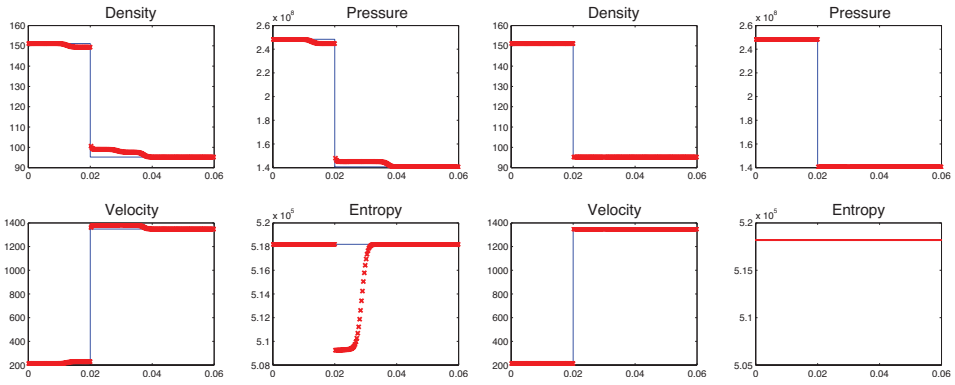

FIGURE 4. Computed and exact solutions corresponding to interface data (3.3): conservative formulation (left) and hybrid formulation (right)

3. Numerical Results - System (1.7)

In this section we present numerical results for the reduced system (1.7) corresponding to the case of a stationary porosity jump and incompressible solid phase. The numerical method in all tests is a Roe-type upwind scheme [**PLR**]

$$W_j^{n+1} = W_j^n - \frac{\Delta t}{\Delta x}\left\{A^+_{j-\frac{1}{2}}\left(W_j^n - W_{j-1}^n\right) + A^-_{j+\frac{1}{2}}\left(W_{j+1}^n - W_j^n\right)\right\} \tag{3.1}$$

with

$$A^+\Delta W = \sum_k \alpha_k \lambda_k^+ r_k \ , \ \lambda_k^+ = \max\left(0,\ \lambda_k\right)$$

$$A^-\Delta W = \sum_k \alpha_k \lambda_k^- r_k \ , \ \lambda_k^- = \min\left(0,\ \lambda_k\right)$$

and

$$\bar{\rho} = \sqrt{\rho_L \rho_R}$$

$$\bar{u} = \frac{\sqrt{\rho_L}u_L + \sqrt{\rho_R}u_R}{\sqrt{\rho_L} + \sqrt{\rho_R}} \qquad \bar{h} = \frac{\sqrt{\rho_L}h_L + \sqrt{\rho_R}h_R}{\sqrt{\rho_L} + \sqrt{\rho_R}}$$

$$\overline{c^2} = (\gamma - 1)\left(\bar{h} - \frac{1}{2}\bar{u}^2\right) \qquad \bar{s} = \frac{s_L + s_R}{2}$$

The CFL number and the grid size are noted in the examples.

Figure 3 shows the computed and exact solutions for the Riemann problem considered in [**CAL**], using CFL number 0.8 and a 2000 point grid. For $U = (\rho, u, p)$, initial data is given by

$$\begin{aligned} U_L &= (1.6934 \times 10^2, 0, 2.96 \times 10^8)^T \\ U_R &= (7.6278 \times 10^{-1}, 0, 1.0 \times 10^5)^T \end{aligned} \tag{3.2}$$

corresponding to a rarefaction wave that straddles the jump in porosity, a contact discontinuity and a shock. In this example, $\phi_L = 1$, $\phi_R = 0.25$ and $\gamma = 1.23$. The computation on the left, based on the conservative formulation, is in noticeable

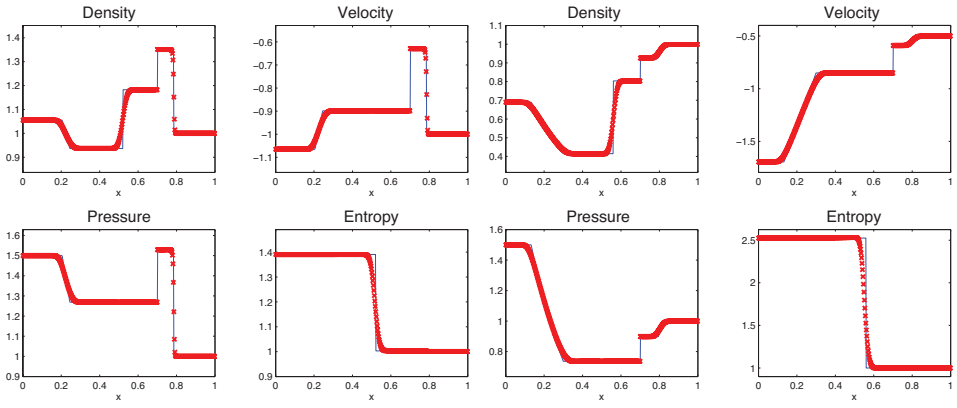

FIGURE 5. Computed and exact solutions corresponding to initial data (3.4) (left) and (3.5) (right)

error (see also [**CAL**]). Visibly, the entropy fails to stay constant across the porosity jump, the solution appears to jump incorrectly across the porosity change yielding an incorrect solution. Figure 3 on the right shows the same computation based on the hybrid formulation which reverts back to the nonconservative formulation using the entropy equation (2.1) across the porosity jump. This formulation clearly recognizes and respects interface data, and yields the correct jump in the solution.

The initial data in Figure 4 correspond to exact interface data extracted from the Riemann problem in the previous example

$$\begin{aligned} U_L &= (1.5113 \times 10^2, 2.1231 \times 10^2, 2.4836 \times 10^8)^T \\ U_R &= (9.5199 \times 10^1, 1.3482 \times 10^3, p_R = 1.4067 \times 10^8)^T \end{aligned} \tag{3.3}$$

with ϕ_L, ϕ_R and γ as above. It illustrates the failure of the conservative formulation to keep the entropy constant across the porosity jump, leading to erroneous waves structure. Using the entropy equation across the porosity jump and the conservative formulation everywhere else makes it possible to recognize and respect the interface data and produces a clean and error free solution.

Figure 5 shows the computed solution by the hybrid scheme for two more Riemann problems, both corresponding to $\phi_L = 1$, $\phi_R = 1.25$ and $\gamma = 1.4$. On the left, the solution corresponding to the initial data

$$\begin{aligned} U_L &= (1.0555, -1.0651, 1.5)^T \\ U_R &= (1.0, -1.0, 1.0)^T \end{aligned} \tag{3.4}$$

producing a left going rarefaction, and a right going shock; on the right, the solution corresponding to the initial data

$$\begin{aligned} U_L &= (6.894 \times 10^{-1}, -1.6941, 1.5)^T \\ U_R &= (1.0, -0.5, 1.0)^T \end{aligned} \tag{3.5}$$

producing a left and right moving rarefactions. The CFL number is 0.8 and the grid has 400 points. Again, the jump conditions across the interface are captured

very well, and the computed solutions are in excellent agreement with the exact solutions, also shown.

4. Numerical Results - BN system (1.1)

We now generalize this computational framework to the full Baer-Nunziato system (1.1). The jump conditions across the porosity jump are

$$[u_s] = 0\ , [\eta_g] = 0\ ,\ [\eta_s] = 0\ ,\ [Q] = 0\ ,\ [P] = 0\ ,\ [H] = 0\ .$$

Here $Q = \phi_g \rho_g v_g$ is the gas mass flux, $H = \frac{1}{2} v_g^2 + \frac{c_g^2}{\gamma - 1}$ is the gas enthalpy and $P = \phi_g p_g + \phi_s p_s + \phi_g \rho_g v_g^2$ is the sum of phase momenta fluxes in the frame of reference of the compaction wave moving with speed u_s, here $v_g = u_g - u_s$.

We have implemented the following hybrid strategy:

(i) Away from the compaction wave, solve for the conservative variables

$$W^C = (\phi_g \rho_g,\ \phi_g \rho_g u_g,\ \phi_g E_g,\ \phi_s \rho_s,\ \phi_s \rho_s u_s,\ \phi_s E_s,\ \phi_s)\ ;$$

(ii) Across the compaction wave, solve for the nonconservative variables

$$W^{RI} = (u_s,\ \eta_g,\ \eta_s,\ Q,\ P,\ H,\ \phi_s)\ .$$

The eigenvectors for the conservative system are essentially the eigenvectors of the two Euler subsystems and an additional eigenvector corresponding to the compaction wave (see for example [**CAL, AW2**]). We note that the eigenvector corresponding to the compaction wave does not play an important role in the present context since the conservative formulation is used only away from the compaction wave, where the porosity does not vary and the corresponding wave strength is zero. The eigenstructure of the nonconservative system based on W^{RI} is

$$R = \begin{pmatrix} 0 & 0 & 0 & -1 & 0 & 0 & -1 \\ 0 & 1 & 0 & 0 & 0 & 0 & 0 \\ 0 & 0 & 0 & 0 & 1 & 0 & 0 \\ 1 & -v_g \tilde{p}_g / \eta_g c_g^2 & 1 & \tilde{\rho}_g & 0 & 0 & \tilde{\rho}_g \\ v_g - c_g & -v_g^2 \tilde{p}_g / \eta_g c_g^2 & v_g + c_g & 2\tilde{\rho}_g v_g + c_s \tilde{\rho}_s & 0 & 0 & 2\tilde{\rho}_g v_g - c_s \tilde{\rho}_s \\ -c_g / \tilde{\rho}_g & \tilde{p}_g / (\gamma - 1) \eta_g \tilde{\rho}_g & c_g / \tilde{\rho}_g & v_g & 0 & 0 & v_g \\ 0 & 0 & 0 & 0 & 0 & 1 & 0 \end{pmatrix}$$

$$\Lambda = diag\,(u_g - c_g, u_g, u_g + c_g, u_s - c_s, u_s, u_s, u_s + c_s)\,.$$

Here we used the abbreviated notation $\tilde{(\ \cdot\ )} = \phi(\ \cdot\ )$ to denote the respective physical quantities scaled by the porosity. Again, the method used in the following examples is a Roe-type upwind scheme (3.1).

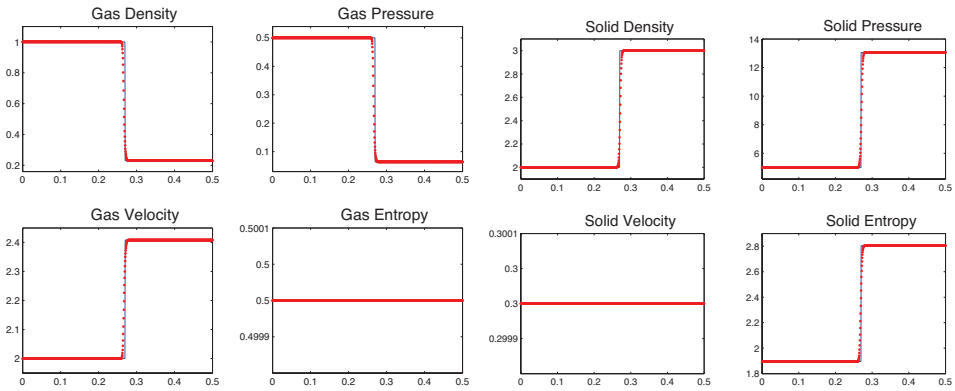

FIGURE 6. Computed and exact solutions corresponding to initial data (4.1): Gas phase (left) and Solid phase (right) by the hybrid formulation

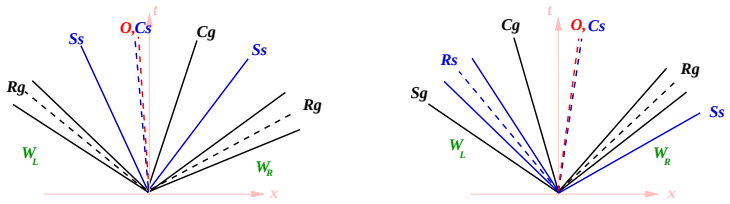

FIGURE 7. Schematic of solution corresponding to initial data (4.2) (left) and to initial data(4.3) (right).

We use U to denote ($\rho_g, u_g, p_g,\ \rho_s, u_s, p_s, \phi_s$) and consider first the Riemann problem for the initial data

$$\begin{aligned} U_L &= (1, 2, 0.5, 2, 0.3, 5, 0.8)^T \\ U_R &= (0.2304, 2.4082, 0.0640, 3, 0.3, 13.0547, 0.3)^T \end{aligned} \tag{4.1}$$

corresponding to a single moving compaction wave. The CFL number is 0.8, the grid size is 400 points, and $\gamma = 1.4$. Figure 6 shows the results by the hybrid formulation which is conservative everywhere except across the compaction wave where it reverts to the nonconservative formulation based on the Riemann Invariants. The results illustrate clearly that the interface data is recognized and respected, and no errors are produced.

The following initial data (see [**CAL**])

$$\begin{aligned} U_L &= (5.71, -0.75, 6.36, 0.553, -0.0553, 0.4527, 0.3)^T \\ U_R &= (2.02, 0.86, 1.87, 1.264, -0.115, 1.1234, 0.7)^T \end{aligned} \tag{4.2}$$

correspond to the Riemann solution depicted in the schematic in Figure 7 (left).

Figures 8 and 9 show the computed and exact solutions by the conservative formulation and the hybrid formulation respectively.

Finally, the solution for the Riemann problem for the initial data (see [**SWK**])

$$\begin{aligned} U_L &= (0.2, 0, 0.3, 1, 0, 1, 0.8)^T \\ U_R &= (1, 0, 1, 1, 0, 1.01, 0.3)^T \end{aligned} \tag{4.3}$$

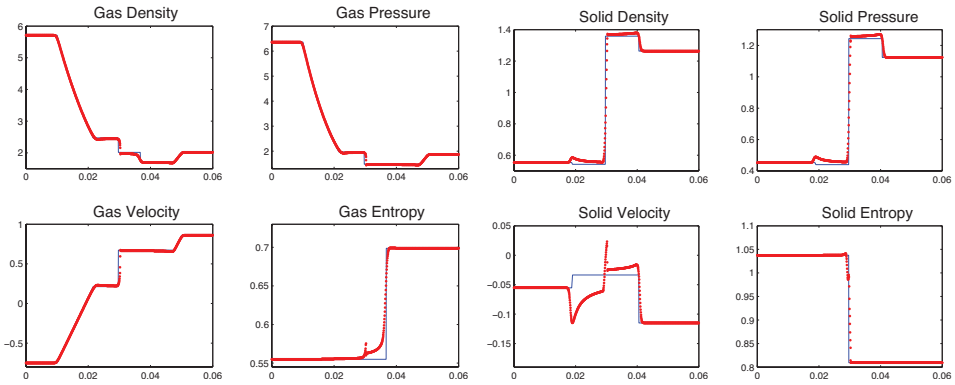

FIGURE 8. Computed and exact solutions corresponding to initial data (4.2): Gas phase (left) and Solid phase (right) by the conservative formulation

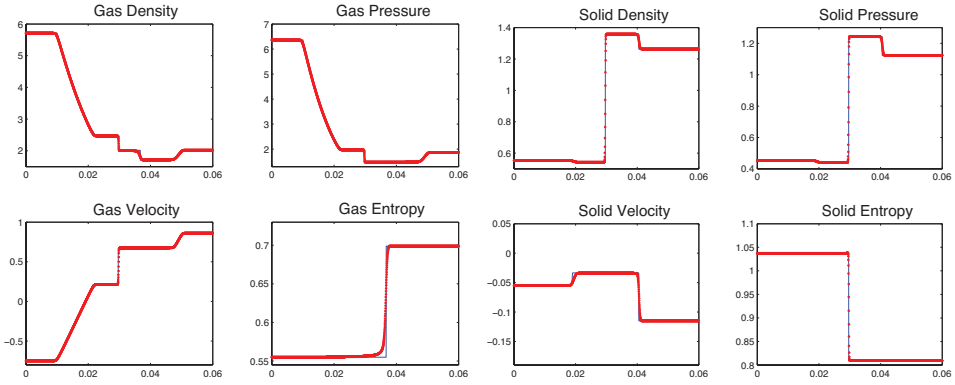

FIGURE 9. Computed and exact solutions corresponding to initial data (4.2): Gas phase (left) and Solid phase (right) by the hybrid formulation

is depicted by the schematic in Figure 7 (right). Computed and exact solutions by the hybrid formulation are shown in Figure 10, and are in very good agreement.

5. Summary

The BN system (1.1) with piecewise constant porosities describes two decoupled Euler sub-sysetms connected via a set of jump conditions across a moving internal boundary called a compaction wave. Numerical methods based on the conservative formulation of the system may produce incorrect jump in solutions across the interface. We have presented a hybrid strategy for the solution of the BN system, which reverts to a formulation based on the set of Riemann Invariants across the moving interface. The formulation trivially recognizes and respects interface data, and is well suited for computing propagating compaction waves. The merits of the hybrid approach have been demonstrated on a variety of shock tube problems for the full BN system (1.1) and for the reduced system (1.7) corresponding to the special case where the interface is stationary and the solid phase assumed incompressible.

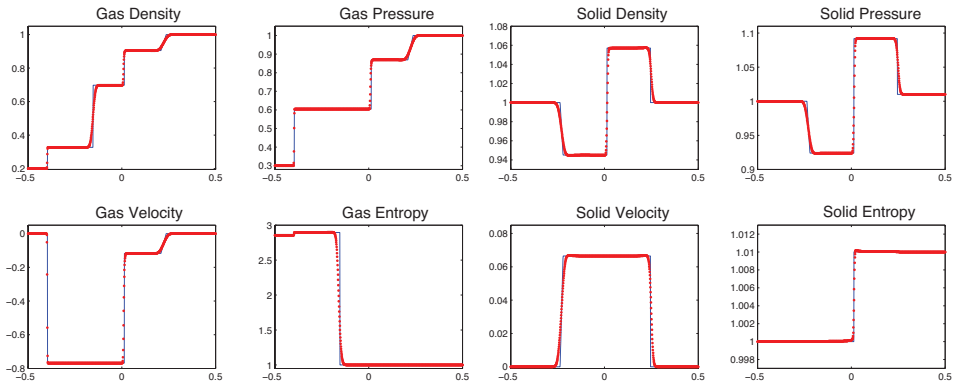

FIGURE 10. Computed and exact solutions corresponding to initial data (4.3): Gas phase (left) and Solid phase (right) by the hybrid formulation

References

[AK] R. Abgrall and S. Karni, *Computations of Compressible Multifluids*, *Journal of Computational Physics*, **169**, 594-623 (2001).

[AW1] N. Andrianov and G. Warnecke, *On the solution to the Riemann problem for compressible flow in a duct*, *SIAM Journal on Applied Mathematics*, **64**, 878-901 (2004).

[AW2] N. Andrianov and G. Warnecke, *The Riemann problem for the Baer-Nunziato two phase flow model*, *Journal of Computational Physics*, **195**, 434-464 (2004).

[BN] Baer and Nunziato, *A two phase mixture theory for the deflagration to detonation transition (DDT) in reactive granular materials*, *Journal of Multiphase Flows*, **12**, 861-889 (1986).

[CAL] C.A. Lowe, *Two-phase shock tube problems and numerical methods of solution*, *Journal of Computational Physics*, **204**, 598-632 (2005).

[GR] G. Russo, *Central schemes for conservation laws with application to shallow water equations, in: S. Rionero, G. Romano (Eds.), Trends and Applications of Mathematics to Mechanics: STAMM 2002, Springer Verlag, Italia SRL, 2005*, 225-246.

[NXS] S. Noelle, Y. Xing, C. Shu, *High-order well-balanced finite volume WENO schemes for shallow water equation with moving water*, **226**, 29-58 (2007).

[PLR] P.L. Roe, *Approximate Riemann Solvers, Parameter Vectors, and Difference Schemes*, *Journal of Computational Physics*, **135**, 250-258 (1981).

[SWK] D.W. Schwendeman, C.W. Wahle and A.K. Kapila, *The Riemann problem and a high-resolution Godunov method for a model of compressible two-phase flow*, *Journal of Computational Physics*, **212**, 490-526 (2006).

DEPARTMENT OF MATHEMATICS, UNIVERSITY OF MICHIGAN, ANN ARBOR, MI 48109
E-mail address: karni@umich.edu

DEPARTMENT OF MATHEMATICS, UNIVERSITY OF MICHIGAN, ANN ARBOR, MI 48109
E-mail address: gerahdez@umich.edu